DOPING- AND CARRIER CONCENTRATION PROFILE CHARACTERISATION OF HIGHLY PHOSPHORUS-DOPED EMITTERS

S. Werner, U. Belledin, A. Kimmerle, A. Fallisch, A. Wolf, D. Biro
Fraunhofer Institute for Solar Energy Systems (ISE)
Heidenhofstrasse 2, D-79110 Freiburg, Germany
Phone: +49 (0)761–4588–5762, Fax: +49 (0)761–4588–9250, E-mail: sabrina.werner@ise.fraunhofer.de

ABSTRACT: In this work we use Secondary Ion Mass Spectrometry (SIMS), Spreading Resistance Analysis (SRA), Stripping Hall (SH) and Electrochemical Capacitance Voltage (ECV) measurements to analyse different phosphorus-diffused emitters. Such data permit the detailed characterisation of the emitter and facilitate an optimisation of the diffusion process. The measurement techniques provide depth resolved information about the phosphorus concentration and the conductivity as well as the electron concentration and mobility. We include an overview of the different measurement techniques. A comparison of the obtained profiles confirms the presence of electrically inactive phosphorus and demonstrates differences in the surface concentration and the p-n-junction depth, which can be mainly attributed to measurement artefacts. However, a good agreement of all techniques is found.
Keywords: Doping, characterisation, diffusion

1 INTRODUCTION

A comprehensive emitter characterisation requires the depth-resolved determination of both the doping- and the carrier concentration as well as the carrier mobility. Such data is important for optimisation of highly efficient silicon solar cells, e.g. for the quantitative modelling of emitter dark saturation current densities J_{0e} [1, 2]. Moreover, selective emitter structures consisting of a local highly doped emitter underneath the grid fingers currently enter the market, demanding a comprehensive characterisation of highly doped emitters. On the other hand novel cell concepts like the emitter wrap-through (EWT) cell concept use deeper emitters to avoid shunting effects and enable a sufficient conductivity.

The different cell concepts have different requirements on the emitter. Therefore an extensive emitter analysis is essential. The emitter dark saturation current density J_{0e} contains information on the emitter recombination and thus the open circuit voltage potential of the device. Quasi Steady State Photoconductance (QSSPC) measurements [3] enable the determination of J_{0e} [4, 5] from the effective lifetime τ_{eff}. A high J_{0e} is often attributed to a high dopant concentration at the surface [6]. Therefore doping- and carrier concentration profiles are necessary to attain knowledge about the amount of dopants in excess of the equilibrium concentration of electrically active dopants. Precipitation of large SiP particles [7, 8], which takes place in the most heavily doped regions, increases the emitter recombination [6].

Several measurement techniques are available for emitter profiling obtaining different information, each having different assets, drawbacks and requirements. A common technique for emitter profile characterisation is Secondary Ion Mass Spectrometry (SIMS) which can be used to obtain a depth profile of chemical doping concentration.

In contrast, approaches based on conductance measurements like Spreading Resistance Analysis (SRA) and Stripping Hall (SH) technique yield the depth-resolved resistivity. Both methods deal with electrical resistivity and not with counting of atoms. Equation (1) describes the relationship between resistivity ρ and carrier concentration n for a homogeneously doped material,

$$\rho = \frac{1}{n e \mu_C} \qquad (1)$$

Here n is the carrier concentration, e is the elementary charge and μ_C is the majority carrier conductivity mobility.

Apparent from Eq. (1), the conversion of the resistivity data into a carrier concentration profile requires the knowledge of the carrier mobility, which in turn depends on the carrier concentration. Suitable mobility models are found in the literature [9-14], which are used for the SRA measurement. The SH technique yields the Hall mobility by Hall measurements.

Finally, the Electrochemical Capacitance Voltage (ECV) technique gives direct access to the carrier concentration profile. However, care must be taken to correct for measurement artefacts [15]. Furthermore, ECV is not suited for high doping concentrations because the range for the applied bias voltage is very small [16].

The aim of this work is to review and demonstrate the capabilities and limits of the different techniques and to gain a consistent overall picture regarding the depth dependent concentration of electrically active phosphorus and the electron conductance mobility in phosphorus-doped emitters.

2 MEASUREMENT TECHNIQUES

2.1 Secondary Ion Mass Spectrometry (SIMS)

A SIMS measurement gives the chemical composition of the samples with very high accuracy. Using sputtering for material removal, it is possible to obtain a depth profile with a resolution of ~1 nm. However, accurate reference samples are needed to calibrate the detectors for each measurement which makes this technique rather expensive. As the full amount of phosphorus is detected by this measurement, it cannot be distinguished between the amount of electrical

active and inactive phosphorus. The uncertainty in the concentration is estimated to be 10 %.

A Cameca imS4f-E6 is used in this work with a 14.5 keV Cs^+ primary ion beam at an oblique angle of incidence.

A theoretical limit of the electrical active phosphorus can be calculated from the known diffusion temperature using the value determined by Solmi et al. [7]

$$n_e = 1.3 \cdot 10^{22} \cdot \exp\left(-0.37 / kT\right) cm^{-3} \qquad (2)$$

Here k denotes the Boltzmann constant and T is the temperature of the last high-temperature step for forming the emitter The equilibrium concentration from Eq. (2) has to be distinguished from the saturation limit of solved phosphorus which is determined by

$$C_{sat} = 2.45 \cdot 10^{23} \cdot \exp\left(-0.62 / kT\right) cm^{-3} \qquad (3)$$

Above this concentration limit phosphorus exists as SiP precipitates [7].

2.2 Spreading Resistance Analysis (SRA)

The spreading resistance is measured with SRA. The values for the spreading resistance are converted into resistivity by applying a calibration chart [17]. In this way, a resistivity versus depth profile is obtained. Then carrier mobility values are used to calculate the dopant concentration according to Eq. (1). The literature provides a number of models and parameterisations for the carrier mobility [9-14]. Especially in the high doping range the individual models for the electron mobility deviate up to a factor of three, making the result strongly dependent on the chosen mobility model. In addition, the system must be periodically calibrated by known standards. A smooth surface is very important because a high surface roughness leads to high errors on the measured resistance values. The strength of SRA lies in its ability to profile a layer without depth limitation. Moreover, besides the resistivity, the doping type (e.g. p- or n-type) is determined.

SRA quotes relative mean errors of 3% for depth and 20% for carrier concentration restricted by the measurement technique.

2.3 Stripping Hall measurement (SH)

The SH technique measures the sheet conductivity σ_s and the Hall coefficient R_s by van der Pauw measurements [18]. A depth profile is obtained by gradually removing layers of the material by anodisation and etching procedures. With equation

$$n(x) = \frac{r}{q}\left(\frac{d\sigma_s}{dx}\right)^2 \left(\frac{d\left(R_s \sigma_s^{\ 2}\right)}{dx}\right)^{-1}$$
$$\mu_H(x) = \frac{d\left(R_s \sigma_s^{\ 2}\right)}{dx}\left(\frac{d\sigma_s}{dx}\right)^{-1} \qquad (4)$$

the carrier concentration $n(x)$ and the Hall mobility $\mu_H(x)$ (x being the depth) can be obtained by the SH measurement where the mobility is the Hall mobility μ_H. However, the conversion of the resistivity profile into a carrier concentration profile requires the knowledge of the carrier conductivity mobility μ_C, which is linked to the Hall mobility μ_H by the scattering factor $r = \mu_H/\mu_C$. The factor r depends on the type of scattering mechanism which must be known for the used material. In our work r is assumed to be unity. In the literature differing values of r are found that range from 1.18 to 1.93 for a high dopant concentration [19, 20]. This assumption generally introduces an error less than 40 %.

One disadvantage of this method is its time-consuming and tedious sample preparation. The measurement does not work in the depletion region because of missing mobile carriers. In this region, resistivity and Hall measurements are no longer possible [21]. For heavily doped material which cannot be measured by *C-V* measurements the SH technique is an inexpensive alternative.

The measurements were performed with the Stripping Hall profiler Bio-Rad HL 5900 on a van der Pauw (VDP) structure [22]. The sample is mounted onto a sample holder (see Figure 1). The VDP pattern is contacted on the edges. An ohmic contact is formed by using a Ga/In eutectic alloy. For the measurement all conductive paths on the sample holder, apart from the sample top surface, must be electrically isolated from the solutions. For this purpose a free flowing silicone rubber compound is used.

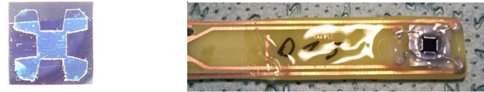

Figure 1: Etched VDP structure (left) and a sample mounted onto a sample holder (right).

By chemical etching, thin layers of the sample are removed. For a well-controlled removal anodic oxidation is a reliable approach. During anodic oxidation a current is induced from an electrode to the semiconductor through an electrolyte (90 % ethylenglycol, 10 % H_2O, 0.05 M KNO). An oxide is grown consuming ~10 nm of silicon. Subsequently the oxide is removed in hydrofluoric acid. This procedure is repeated until the desired depth is reached.

2.4 Electrochemical Capacitance Voltage profiling (ECV)

The ECV technique is based on the fact that the width of a reverse-biased space charge region depends on the applied voltage. All calculations are based on equation

$$n(x) = -\frac{C^3}{\varepsilon_0 \varepsilon_r e A^2 \frac{dC}{dV}} = \frac{2}{\varepsilon_0 \varepsilon_r e A^2 \frac{d\left(1/C^2\right)}{dV}} \qquad (5)$$

Here n is the carrier concentration, C is the capacitance, A is the etch area, V is the externally applied potential, e is the elementary charge and ε_0 and ε_r are the permittivity for free space and the relative permittivity of the material, respectively. The doping density is obtained from the slope $d(1/C^2)/dV$ of a $1/C^2$ versus V plot [16].

Depth profiling is achieved by electrochemically etching the semiconductor between the capacitance measurements. The doping concentration is calculated

from the ECV measurement assuming a fixed etch area which is defined by the sealing ring area of the equipment. The size of the etch crater is the main source of errors in the ECV measurement even if the etch area is fixed. By measuring the geometry of the etch crater after the ECV measurement it can be found that the contact area differs from the sealing ring area [15]. Moreover it is required to confirm the depth of the crater e.g. by a surface profiler.

3 EXPERIMENTAL

For the emitter profiling boron-doped shiny etched float zone (FZ) wafers with a resistivity of ~1 Ωcm and boron-doped polished Cz wafers with a resistivity of ~0.5 Ωcm for the SRA measurements where a flat surface is advantageous are used. A tube furnace $POCl_3$-diffusion forms different emitter profiles with different sheet resistances. The sheet resistance is measured by means of inductive coupling [23].

Figure 2 illustrates the process sequence of the experiment.

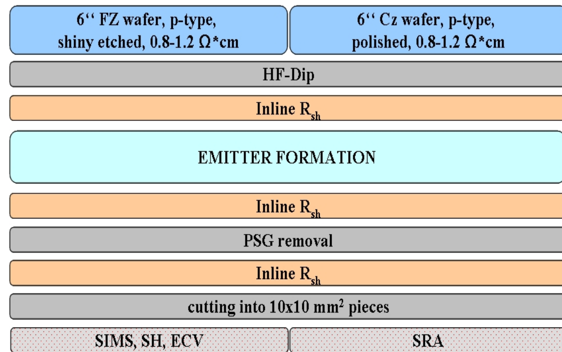

Figure 2: Process flow for sample preparation and characterisation.

Before the diffusion process a resistance measurement yields the resistance of the substrate. A second measurement after the diffusion allows the determination of the emitter sheet resistance [23]. After removing the phosphorus silicate glass (PSG) the wafers are cut into smaller pieces and neighbouring samples are analysed using the different measurement techniques described in Section 2.

4 RESULTS AND DISCUSSION

4.1 Industrial Emitter

An emitter used for screen-printed silicon solar cells with aluminium back surface field has been characterised. The sheet resistance R_{sh} is 82 Ω/sq. The depth profile is shown in Figure 3. For SIMS measurement, the profile shows a peak concentration of $1.2 \cdot 10^{21}$ cm^{-3} near the surface and a junction depth of about 0.35 µm. It is supposed that the high surface concentration is a measurement artefact or it may possibly be supersaturated phosphorus. By calculating the average of the concentrations between 0.01 µm und 0.02 µm a surface concentration of $4.4 \cdot 10^{20}$ cm^{-3} can be found.

SIMS provides the total amount of phosphorus concentration. Above the equilibrium carrier concentration n_e the phosphorus atoms are in non ionized forms [7]. For the used emitter, which is diffused at 833 °C, n_e of $2.68 \cdot 10^{20}$ cm^{-3} is calculated from Eq. (2).

A sample of the same diffusion was also measured by SRA. The result can be seen in Figure 3 as well. Klaassen's mobility model [13, 14] was used to calculate the carrier concentration from the measured resistivity with Eq. (1).

SIMS and SRA profiles show good agreement between depth of 0.05 µm and 0.25 µm. Typically, SIMS and SRA differ in the obtained junction depth which is about 0.27 µm for SRA. SRA predicts lower junction depth. Here, the carrier concentration deviates from the dopant concentration due to so-called carrier spilling [24].

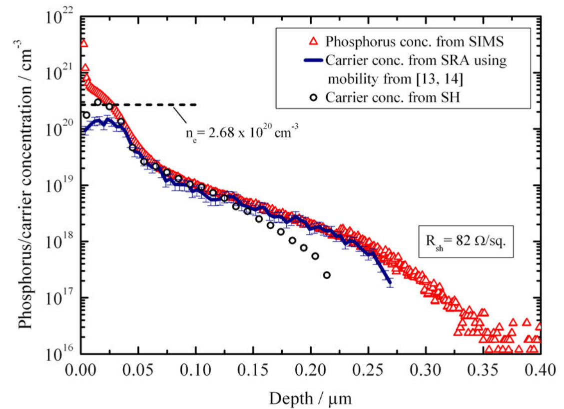

Figure 3: SIMS, SRA and SH profiles of an industrial emitter and the equilibrium carrier concentration n_e of the electrically active dopant published in [7].

The predicted surface concentration also differs between SIMS and SRA measurement. The values determined by SRA are much lower. At high concentrations (> $1 \cdot 10^{19}$ cm^{-3}) there is only a small gradient for the resistivity which results in high signal-to-noise ratio in spreading resistance measurement. Moreover, the different mobility models deviate strongly for high doping level making the surface concentration values dependent on the chosen model. It should also be remembered that SIMS measures the total phosphorus concentration while SRA gives the carrier concentration, which might be converted into a concentration of electrically active phosphorus by means of a Poisson solver [25]. However in our case we do not perform a transformation of the data.

The profile of the industrial emitter obtained by SH can also be seen in Figure 3. The data is in good agreement with SIMS and SRA measurements in the range from 0.05 µm to 0.15 µm. Discrepancies appear for values higher than 0.15 µm and in the surface region.

At 0.2 µm depth the SH method cannot measure the Hall coefficient anymore because of missing carriers within the space charge region [21].

The measured surface concentration is in good agreement to the literature value for the equilibrium concentration of the electrically active dopant n_e given by $2.68 \cdot 10^{20}$ cm^{-3}. The values extracted from SRA are lower. Both measurements differ in surface carrier concentration

because of the usage of a carrier concentration-resistivity relationship for SRA values valid for perfect crystals [12].

4.2 High Efficiency Emitter

The following deals with an emitter which is of interest for high efficiency solar cells with selective emitter. The emitter is driven in by a subsequent oxidation to obtain a low surface concentration. The dopant profile was measured with all four techniques mentioned above (see Figure 4).

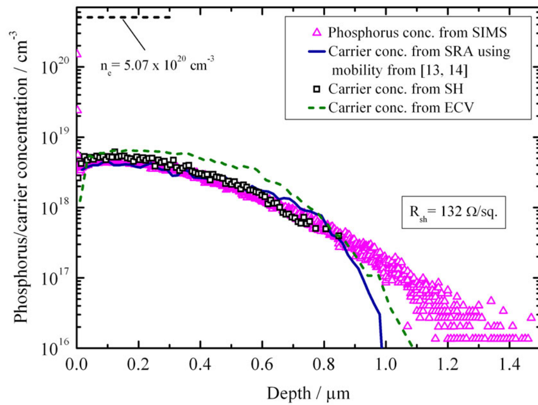

Figure 4: SIMS, SRA, SH and ECV profiles of a high efficiency emitter.

The SIMS, SRA and SH profiles show a good agreement, again except for the junction depth because of the mentioned measurement limitations of each technique. The surface concentration of sample F does not deviate for the various measurement methods. As the equilibrium concentration n_e of the electrically active dopant is a factor 50 higher than the surface concentration, all measurement techniques give the electrically active phosphorus content which in this region is equivalent to the carrier concentration.

For ECV measurement, it is essential to verify the etch depth and the crater size area [15], which is usually assumed to be equal to the size of the sealing ring. The carrier concentration is dependent on the area to the square as can be seen in Eq. (5). The verification was done by a surface profiler. The analysis of crater dimensions leads to a correction factor of 1.25 in depth and 1.07 in concentration. The corrected ECV profile is illustrated in Figure 4.

The carrier concentration is higher for ECV than the concentration obtained by the other techniques. It can be supposed that this phenomenon is caused by side wall effects. As the etch depth becomes larger, the area of the side wall of the etch crater increases. This side wall area contributes to the capacitance of the total crater surface [16]. The side wall concentration is higher than the concentration at the crater bottom. Therefore the deviation between the ECV and the other profiles increases with depth. At the surface, all measurement techniques are in good agreement.

4.3 Carrier Mobility

In Figure 5, the conductivity mobility model of Thurber [12] which is sometimes used for SRA and the Hall mobility obtained by SH are compared with Klaassen's mobility model [13, 14] and with the device simulation program PC1D [9].

Within experimental errors, the model of Klaassen and the measured Hall mobility show a good agreement. There is a mean deviation of 10.9 %. Note that the model of Klaassen is based on the results from Masetti [11] who measured the Hall mobility and assumed a Hall scattering factor r of unity. For Thurber's mobility values, there is a mean deviation of 26.9 % from the physical model. The mobility decreases for Klaassen [13, 14] compared to Thurber [12] or PC1D [9] at high carrier concentration as Klaassen assumes carrier scattering by impurities with more than one electron charge and a cluster concentration [13]. In this range, Klassen's mobility model is the most suitable one.

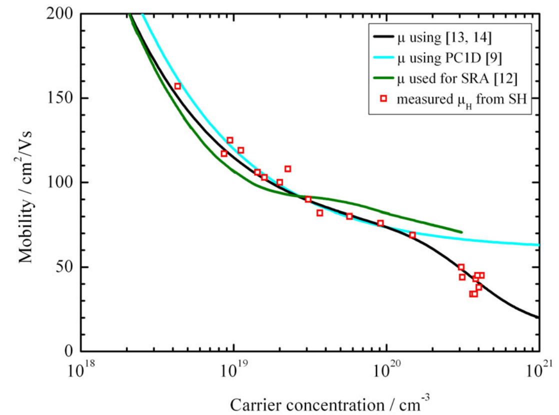

Figure 5: Mobility versus carrier concentration obtained by SH in comparison to the mobility model by Klaassen [13, 14], PC1D [9] and Thurber [12].

5 CONCLUSION

We show that each of the presented profiling techniques performs very good in order to profile dopant or carrier concentration. The choice of one technique depends on the demanded physical quantity in each specific case. SIMS measures the total dopant concentration and must be used if knowledge about inactive and supersaturated phosphorus is needed. If the amount of inactive phosphorus is not of interest or not at hand, SRA, SH and ECV are satisfying alternatives, since they give the carrier concentration, where a mobility model is required in the case of SRA. These methods can be also applied additionally to SIMS to verify the theoretical limit from Eq. (2).

SRA has no depth limitation, which makes this technique valuable for very thick samples. However, care must be taken regarding the surface concentration and the p-n-junction depth. A suitable mobility model has to be used to calculate the phosphorus concentration. One disadvantage of this method is that polished samples have to be used which are rather expensive.

The strength of SH especially lies in the ability to yield the Hall mobility and a carrier concentration profile without the need of a mobility model. The measured carrier mobility values are in a good agreement with Klaassen's mobility model. However, a scattering factor must be assumed to convert the Hall mobility into a conductivity mobility. SH can also be used to verify the calculated electrical active phosphorus concentration n_e.

Due to missing mobile carriers the Hall measurement is not possible in the depletion region, which limits the correct determination of p-n-junction depth. If the whole amount of phosphorus is electrically activated and the junction depth is minor importance, this method is a suitable profiling technique.

ECV depends on many parameters such as measurement voltage, electrolyte concentration or dissipation factor. As the supposed width and depth of the etch crater is the main source of error in this measurement, it has to be measured after the profiling. For phosphorus emitters with a high surface concentration this method is not very suitable Nevertheless, the ECV technique is an effective method for profiling of emitters.

For a purpose of a full understanding of the dopant activation phenomenon, more developed analysis must be performed.

6 ACKNOWLEDGEMENTS

We gratefully acknowledge the technical support by the PV-TEC co-workers. This work is supported by the German Federal Ministry of Environment, Nature Conservation and Nuclear Safety under contract 0329849B.

7 REFERENCES

[1] P. P. Altermatt, J. O. Schumacher, A. Cuevas, S. W. Glunz, R. R. King, G. Heiser, and A. Schenk, "Numerical modeling of highly doped Si:P emitters based on Fermi-Dirac statistics and self-consistent material parameters", *Journal of Applied Physics*, **vol. 92**, pp. 3187-97, 2002.

[2] A. Cuevas, R. A. Sinton, and M. Stuckings, "Determination of Recombination Parameters in Semiconductors from Photoconductance Measurements", *presented at Proceedings of the 1996 Conference on Optoelectronic and Microelectronic Materials and Devices*, Canberra, ACT, Australia, 1996.

[3] R. A. Sinton, A. Cuevas, and M. Stuckings, "Quasi-steady-state photoconductance, a new method for solar cell material and device characterization", *presented at Proceedings of the 25th IEEE PVSC*, Washington DC, USA, 1996.

[4] C. Reichel, F. Granek, J. Benick, O. Schultz-Wittmann, and S. W. Glunz, "Comparison of emitter saturation current densities determined by quasi-steady-state photoconductance measurements of effective carrier lifetimes at high and low injections", *presented at Proceedings of the 23rd EU PVSEC*, Valencia, Spain, 2008.

[5] A. B. Sproul, "Dimensionless solution of the equation describing the effect of surface recombination on carrier decay in semiconductors", J*ournal of Applied Physics*, **vol. 76**, pp. 2851-4, 1994.

[6] P. Ostoja, S. Guerri, P. Negrini, and S. Solmi, "The Effects of Phosphorus Precipitation on The Open-Circuit Voltage in N^+/P Silicon Solar Cells", *Solar Cells*, **vol. 11**, pp. 1-12, 1984.

[7] S. Solmi, A. Parisini, R. Angelucci, A. Armigliato, D. Nobili, and L. Moro, "Dopant and carrier concentration in Si in equilibrium with monoclinic SiP precipitates", *Physical Review B*, **vol. 53**, pp. 7836, 1996.

[8] M. Finetti, P. Negrini, S. Solmi, and D. Nobili, "Electrical properties and stability of supersaturated phosphorus-doped silicon layers", *Journal of the Electrochemical Society: Solid-State Science and Technology*, **vol. 128**, pp. 1313-7, 1981.

[9] D. A. Clugston and P. A. Basore, "PC1D version 5: 32-bit solar cell modeling on personal computers", *presented at Proceedings of the 26th IEEE Photovoltaic Specialists Conference*, Anaheim, California, USA, 1997.

[10] J. M. Dorkel and P. Leturcq, "Carrier mobilities in silicon semi-empirically related to temperature, doping and injection level", *Solid-State Electronics*, **vol. 24**, pp. 821-5, 1981.

[11] G. Masetti, M. Severi, and S. Solmi, "Modeling of carrier mobility against carrier concentration in arsenic-, phosphorus-, and boron-doped silicon", *IEEE Transactions on Electron Devices*, **vol. 30**, pp. 764-9, 1983.

[12] W. R. Thurber, R. L. Mattis, Y. M. Liu, and J. J. Filliben, "The Relationship Between Resistivity and Dopant Density for Phosphorus- and Boron-Doped Silicon", *National Bureau of Standards Special Publication*, 1981.

[13] D. B. M. Klaassen, "A unified mobility model for device simulation - I. Model equations and concentration dependence", *Solid-State Electronics*, **vol. 3**5, pp. 953-9, 1992.

[14] D. B. M. Klaassen, "A unified mobility model for device simulation - II. Temperature dependence of carrier mobility and lifetime. " *Solid-State Electronics*, **vol. 35**, pp. 961-7, 1992.

[15] R. Bock, P. P. Altermatt, and J. Schmidt, "Accurate Extraction of Doping Profiles from Electrochemical Capacitance Voltage Measurements", *presented at Proceedings of the 23rd EU PVSEC*, Valencia, Spain, 2008.

[16] P. Lölgen, "Surface and Volume Recombination in Silicon Solar Cells", Univ. of Utrecht, 1995.

[17] R. Brennan and D. Dickey, "Determination of Diffusion Characteristics Using Two- and Four-Point Probe Measurements", *Solecon Labs Technical Note*.

[18] L. J. v. d. Pauw, "A method of measuring specific resistivity and hall effect of discs of arbitrary shape", *Philips Research Reports*, **vol. 13**, pp. 1-9, 1958.

[19] J. Boussey, "Stripping Hall effect, sheet and spreading resistance techniques for electrical evaluation of implanted silicon layers", *Microelectric Engineering*, **vol. 40**, pp. 275-284, 1998.

[20] A. Schenk, P. P. Altermatt, and B. Schmithüsen, "Physical Model of Incomplete Ionization for Silicon Device Simulation", *presented at SISPAD*, 2006.

[21] Bio-Rad and S. S. Division, "HL5900PC Hall Profiler System", *Operator's Manual*, 1997.

[22] L. J. v. d. Pauw, "A method of measuring resistivity and hall coefficient on lamellae of arbitrary shape", *Philips Technical Review*, **vol. 20**, pp. 220-224, 1958/59.

[23] M. Spitz, U. Belledin, and S. Rein, "Fast Inductive Inline Measurement of the Emitter Sheet Resistance in Industrial Solar Cell Fabrication", *presented at Proceedings of the 22nd EU PVSEC*, 2007.

[24] R. G. Mazur and D. H. Dickey, "A spreading resistance technique for resistivity measurements in Si", *Journal of the Electrochemical Society*, **vol. 113**, pp. 255–259, 1966.

[25] D. H. Dickey, "A Poisson Solver for Spreading Resistance Analysis", *Journal of Vacuum Science & Technologie B*, **vol. 10**, pp. 438, 1992.